Estimation of ice content in mortar based on electrical measurements under freeze-thaw cycle

Yi Wang, Fuyuan Gong, Dawei Zhang, Tamon Ueda

Journal of Advanced Concrete Technology, volume 14 (2016), pp. 35-46

Scientific paper

Estimation of Ice Content in Mortar Based on Electrical Measurements under Freeze-Thaw Cycle

Yi Wang[1], Fuyuan Gong[2], Dawei Zhang[3*] and Tamon Ueda[4]

Received 16 August 2015, accepted 31 January 2016 doi:10.3151/jact.14.35

Abstract

Ice content is an essential factor that affects the internal pressure of cement-based materials during freeze-thaw cycles (FTCs). Since the electrical conductivity of mortar is closely related to its moisture content, it is possible to estimate the ice content based on electrical conductivity variation of mortar. As a result, the ice formation process during FTCs can be monitored. This paper proposed a model to estimate the ice content by applying electrical measurements and clarified the combined effects of temperature and moisture content for electrical conductivity of mortar. The ice content of mortar was estimated with the model by conducting the electrical test. The results are found in acceptable agreement with theoretical results from thermodynamic analysis, and the relationship between ice content and temperature is similar to existing calorimetric test results, which confirm the reliability of the model and the proposed test method.

1. Introduction

Frost damage to concrete is of great concern in cold regions, especially for concrete infrastructure related to transportation (Valenza and Scherer 2007). Many models have been proposed to explain the mechanism of frost damage such as hydraulic pressure (Powers 1945), crystallization pressure (Scherer and Valenza 2005) and cryosuction pressure (Sun and Scherer 2010a). A comprehensive hydraulic model was also developed by Gong *et al.* (2015a) to explain the relationship between internal pressure and deformation of concrete. According to Gong *et al.*'s model, to obtain the internal pressure with freeze-thaw cycles (FTCs), it is rational to apply the sum of the above three pressures. However, all of these models require the information of ice content as a known input, which still cannot be measured confidently during freeze-thaw cycles, even though some studies provide useful information by using differential scanning calorimeter (Johannesson 2010, Sun and Scherer 2010b), but it is limited to pore size from 4nm~100nm and the result would be complicated to interpret if there is solute in the pore liquid since the salt can change the heat flow state in concrete (Kjeldsen and Geiker 2008).

[1]Graduate Student, Lab of Engineering for Maintenance System, Graduate School of Engineering, Hokkaido University. Sapporo, Japan.
[2]Graduate Student, Lab of Engineering for Maintenance System, Graduate School of Engineering, Hokkaido University, Sapporo, Japan.
[3]Associate Professor, College of Civil Engineering and Architecture, Zhejiang University, China.
*Corresponding author, *E-mail*: dwzhang@zju.edu.cn
[4]Professor, Lab of Engineering for Maintenance System, Faculty of Engineering, Hokkaido University, Sapporo, Japan.

Recently, using electrical measurements to investigate the micro-characteristics of cement-based materials has attracted more interest because of its high efficiency and easy application (Spragg *et al.* 2012). It seems also quite promising to use this method to study the frost damage of concrete, especially for the ice formation process (Perron and Beaudoin 2002; Sato and Beaudoin 2011). The electrical conductivity of concrete depends on five factors: porosity, connectivity, chemical composition of pore solution, saturation degree (moisture content) of concrete and temperature (Weiss *et al.* 2012). Generally, when the temperature is decreasing below the freezing point, the content of unfrozen water gradually decreases. According to existing understandings (Whittngton *et al.* 1981; Katsura *et al*. 1996; Sato and Beaudoin 2011; Spragg *et al.* 2013), both temperature and moisture content have a significant influence on the electrical conductivity of concrete. Weiss *et al.* (2012) suggested the relationship between electrical conductivity and degree of saturation of concrete under normal temperatures considering the porosity, connectivity of concrete and chemical composition of the pore solution (modified from the model of Archie (1942) in soil science). Effect of temperature on electrical conductivity of concrete has also been studied by applying Arrhenius's law (Chrisp *et al.* 2001; Liu and Presuel-Moreno 2014). Wang *et al.* (2014, 2015) observed the electrical resistivity change in response to temperature and the change of ice nucleation temperature during FTCs. However, current studies only focused on the effect of either moisture content or temperature on the electrical conductivity of concrete (Villagrán Zaccardi *et al.* 2009). The combined effect of moisture content and temperature on electrical conductivity should be clarified firstly if one wants to monitor the ice formation process reliably based on the electrical measurements.

In terms of estimating ice content based on electrical measurement, Cai and Liu (1998) developed a simple model to predict the ice content by assuming that the electrical resistance of the pore solution is constant and is equal to the electrical resistance of the specimen, however, in reality, the resistance of the specimen varies against the temperature and moisture condition. McCarter *et al.* (2015) also proposed a model to predict the ice content based on electrical measurement with a similar equation to Cai and Liu's, but it considers the effect of temperature on pore solution. Nevertheless, in their study the contributions of porosity and connectivity to the electrical conductivity of the specimen are ignored and the ice formation process is instant rather than continuous. Farnam *et al.* (2015) studied the electrical response of mortar under FTC to detect the phase change. In their study, a damage index based on the ratio of electrical resistivity before and after FTC was used to evaluate the frost damage of mortar with different degrees of saturation. A comprehensive relationship between the ice content and the electrical conductivity of mortar considering the combined effects of moisture and temperature has not been derived.

The purpose of this paper is to derive a rational relationship between the ice content and the electrical conductivity of mortar and to understand the ice formation process in mortar under FTCs based on electrical measurements. A better understanding of combined effects of temperature and degree of saturation on electrical conductivity is to be achieved. In addition to the combined effects, with regard to serious damage of concrete after repeated FTCs, the model is extended to multiple cycles by considering the damage within each cycle. The results of this paper are of significance in predicting the mechanical degradation of concrete under FTCs, as well as life cycle of concrete structures in cold regions. Furthermore, the knowledge of combined effects of temperature and degree of saturation can also be used to improve the understanding of hydration process of cement mortar by electrical monitoring the combined effects of temperature and moisture content.

2. Theoretical model for the combined effects of temperature and moisture content

The degree of saturation is an important factor for electrical conductivity of concrete since it is related to the electrical conductivity of pore solution, water filled porosity and water connectivity, which are the dominant factors of electrical conductivity. Recently, Weiss *et al.* (2012) suggested a saturation function (Eq. (1)) to account for the electrical properties of partially saturated concrete based on the fact that the water filled porosity and water connectivity are proportional to a power law function of degree of saturation, which was originally developed in Archie (1942).

$$\frac{\sigma_c}{\sigma_{cs}} = S^n \tag{1}$$

where σ_c is the electrical conductivity of partially saturated concrete, σ_{cs} is the electrical conductivity of fully saturated concrete, S is the degree of saturation of concrete, n is the saturation coefficient which is determined by two parts, the intrinsic properties of concrete such as porosity and connectivity and chemical composition of pore solution (Based on existing experimental data (Weiss *et al.* 2012), for w/c=0.5, n of mortar approximately equals to 3.5). During freezing, water content loss due to ice formation, concentration and conductivity of the pore solution increases. Since the parameter 'n' is related to pore solution composition which could account for the nonlinear relationship between conductivity and concentration, as discussed in Weiss *et al.* (2012), Eq. (1) can be used to estimate the degree of saturation change based on the change of electrical conductivity.

Temperature also has a significant effect on electrical conductivity of concrete because it can change the mobility of ions. Under high temperature, the ions are more active, consequently the electrical conductivity is higher and vice versa. Generally, researchers consider that the Arrhenius equation (Eqs. (2) and (3)) can be reliable in describing the relationship between electrical conductivity and temperature (for temperature range of 0-50℃), and it is less temperature dependent when the temperature is higher than 50℃(Spragg *et al.* 2013; Chrisp *et al.* 2001; Liu and Presuel-Moreno 2014). Moreover, with regard to recent research results (Panchmatia *et al.* 2014), the equation is also applicable under a temperature of -18℃, therefore, it is possible to use it for investigating ice formation process.

$$\sigma = Ae^{-\left(\frac{E_a}{R_g T}\right)} \tag{2}$$

$$\frac{\sigma}{\sigma_{ref}} = e^{-\left[\frac{E_a}{R_g}\left(\frac{1}{T}-\frac{1}{T_{ref}}\right)\right]} \tag{3}$$

where σ is the electrical conductivity measured at the absolute temperature T (K), σ_{ref} is the conductivity at absolute reference temperature T_{ref}, the measured one and the reference one are the same degree of saturation, A is the nominal conductivity at infinite temperature ($T\rightarrow\infty$) in S/m, E_a is the activation energy for the conduction process in kJ/mol and R_g is the universal gas constant =8.314 J/mol/K.

The activation energy of concrete (E_a) is the parameter that determines the sensitivity of electrical conductivity of concrete with regard to temperature. However, it is not a constant and increases with the decreasing of degree of saturation from existing experimental observations (Chrisp *et al.* 2001). The value of E_a has been reported to range from 16.9 to 42.8 kJ/mol (Liu and Presuel-Moreno 2014). In order to analyze the temperature effect on electrical conductivity of concrete quantitatively and accurately, it is necessary to clarify the relationship between the activation energy and the degree of saturation.

For the above purpose, as derived in the Appendix, the activation energy of partially saturated concrete can be written as the following equations

$$E_{a,s} = -\frac{R_g \ln\left(\frac{\sigma_{T,s}}{\sigma_{ref,s}}\right)}{\frac{1}{T} - \frac{1}{T_{ref}}} \quad (A.7)$$

$$E_{a,p} = E_{a,s} - R_g T_{ref} \ln\left(S^n\right) \quad (A.14)$$

where $E_{a,p}$ is the activation energy of partially saturated concrete for the conduction process and $E_{a,s}$ is the activation energy of fully saturated concrete for the conduction process. $\sigma_{T,s}$ is the electrical conductivity of fully saturated concrete at the absolute temperature T, $\sigma_{ref,s}$ is the electrical conductivity of fully saturated concrete at the reference temperature T_{ref}.

Based on the above equation, the normalized electrical conductivity (see **Fig. 1**) can be calculated as (see detailed derivation in appendix)

$$\frac{\sigma_{T,p}}{\sigma_{ref,s}} = e^{-\left[\frac{E_{a,s} - R_g T_{ref}\ln\left(S^n\right)}{R_g}\left(\frac{1}{T} - \frac{1}{T_{ref}}\right)\right]} \cdot S^n \quad (A.15)$$

By reversing Eq. (A.15), we have the relative content of unfrozen water (the same value as liquid saturation degree during freezing and thawing) as

$$S = \sqrt[n\frac{T_{ref}}{T}]{\frac{\sigma_{T,p}}{\sigma_{ref,s}} \cdot e^{\left[\frac{E_{a,s}}{R_g}\left(\frac{1}{T} - \frac{1}{T_{ref}}\right)\right]}} \quad (4)$$

During freezing the water transforms to ice. Since the conductivity coefficients of ice (solid) and vapor are very low compared to that of water (σ_{liq}=1~20 S/m, $\sigma_{sol}\approx 10^{-9}$ S/m, $\sigma_{vap}\approx 10^{-15}$ S/m (Rajabipour and Weiss 2007) and $\sigma_{ice}\approx 10^{-6}$ S/m (Petrenko 1993)), the conductivity is mostly determined by the conductivity of pore

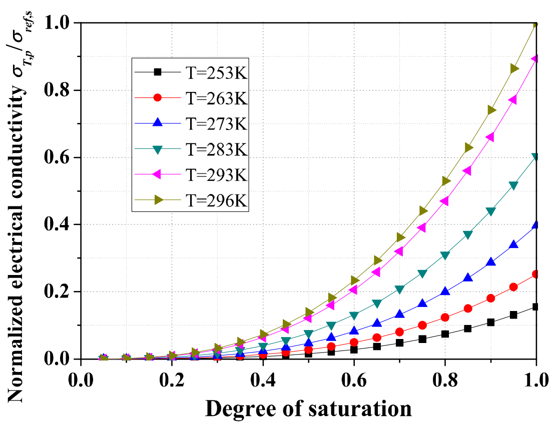

Fig. 1 The relationship between the electrical conductivity and degree of saturation.

solution. Therefore, the degree of saturation can be considered as relative content of unfrozen water. The relative ice content I is then determined as

$$I \approx S_0 - S \quad (5)$$

where S_0 is the initial saturation degree.

In addition, the frost damage may also affect the electrical conductivity by altering the porosity and connectivity of concrete, which makes the accuracy of the calculated ice content with FTCs reduced. However, at this stage, it is very difficult to quantitatively analyze the frost damage based on temperature change. The internal pore pressure in concrete can be calculated by ice formation along with temperature change which could be used for evaluating the damage, but once the damage developed, the ice content estimation would be affected, as a result, the damage cannot be evaluated accurately with temperature. According to Gong *et al.* (2015b), during freezing, damage increases, while during thawing the damage rather remains, therefore a possible simple solution is to differentiate the freezing and thawing process with and without considering damage evolution based on the damage mechanisms difference, respectively. In this case, the estimated ice content for multiple cycles would be more accurate. But this is only a simple approach for understanding the damage effect on ice estimation. In order to analyze the damage development quantitatively based on ice formation, it still needs further investigation. With regard to the damage development during freezing, the referenced electrical conductivity at i cycle may change with temperature after ice formation until it reaches the referenced electrical conductivity at i+1 cycle (see discussion in Section 4.5) since it could be considered as a parameter to evaluate the damage (Farnam *et al.* 2015). Thus, Eq. (4) is extended to the case of repeated freeze-thaw cycles as follows

$$S_{iF} = \sqrt[n\frac{T_{ref}}{T}]{\frac{\sigma_{T,p}}{\sigma_{ref_i,s} + \frac{T-T_F}{T_L - T_F}\left(\sigma_{ref_{i+1},s} - \sigma_{ref_i,s}\right)} e^{\left[\frac{E_{a,s}}{R_g}\left(\frac{1}{T} - \frac{1}{T_{ref}}\right)\right]}} \quad (6)$$

$$S_{iT} = \sqrt[n\frac{T_{ref}}{T}]{\frac{\sigma_{T,p}}{\sigma_{ref_{i+1},s}} e^{\left[\frac{E_{a,s}}{R_g}\left(\frac{1}{T} - \frac{1}{T_{ref}}\right)\right]}} \quad (7)$$

where S_{iF} and S_{iT} are unfrozen water content during freezing and thawing at a certain i cycle, $\sigma_{refi,s}$ and $\sigma_{refi+1,s}$ are the electrical conductivity of fully saturation concrete at the reference temperature before and after the i cycle. T_F is the freezing point and T_L is the lowest temperature (K).

3. Experimental methodology

3.1 Specimen preparation

Mortar specimens were prepared. The mix proportion is based on ACI Committee 211 (1991), in which the coarse aggregate was not included. The w/c ratio is 0.5, water is 207 kg/m^3, cement is 414 kg/m^3 and fine aggregate is 990 kg/m^3. The materials used were Ordinary Portland Cement with density 3.14 g/cm^3, fine aggregate of 1.2 mm or less in size with density 2.67 g/cm^3 and there is no admixture added. After proper mixing, the specimens were cast into ϕ50 mm×100 mm cylinders and cured for 24 hours before demolding. Once the specimens were demolded, they were cured under water for 90 days at room temperature 23±2℃. The cured specimens were oven dried at 105℃ for 24 hours in order to remove the evaporable water. Although there is possibility that the specimens have initial damage when the drying temperature was set 105℃, the oven-drying induced damage is insignificant compared with further frost damage according to the test results of Sicat *et al.* (2013). Therefore, the estimated ice content based on normalized electrical conductivity is still reasonable. Then the specimens were submersed in water until mass was constant to attain full saturation. Finally, the specimens were sealed with polyvinylidene chloride plastic (commonly known as Saran) and vinyl/mastic tape to prevent moisture loss. Before conducting the electrical measurements, the tape and Saran in the end of the cylinder specimen were removed and thus the specimen can contact with sponges.

3.2 Test method

In this test, we adopted end to end AC two point test and referred to the setup of Spragg *et al.* (2011), as shown in **Fig. 2(a)**. The cylinder mortar was placed inside of the environmental chamber, two steel plate electrodes connect with the alligators of a commercial resistivity meter and the ends of the cylinder. The wet sponges, which were saturated with 20%wt NaCl solution to have high conductivity, were used between plate electrodes and cylinder specimen for better contact. Moreover, because the thinner the sponge is, the smaller the resistance would be, the thickness of the sponge in this test is about 2mm which is the thinnest found in the market (see **Fig. 2(b)**). To assure a good contact between electrodes and specimen, which may affect the resistivity measurement significantly, external pressure of 6 kPa was applied as an external mass on the top electrode, as recommended by Newlands *et al.* (2008). Since the direct current causes polarization effect which increases the electrical resistivity, alternating current with a frequency of 1kHz was chosen for measurement, as the optimized frequency confirmed by McCarter *et al.* (2015). The uniaxial resistivity of specimen was measured continuously by the resistivity meter and the data was collected by computer automatically every 3 seconds. Three specimens at the same condition were used for testing and they were measured continuously for hours to get stable values for each designed temperature and obtain the exact value of activation energy of mortar at saturation. The electrodes were sandblasted before each measurement to assure that their resistance is the same for different specimens. The electrical resistance of the sponges was measured first because the resistance of the sponges during the FTCs may influence the total resistance.

3.2.1 Method of calculating the electrical conductivity

Resistance of mortar was calculated based on the method applied by Spragg *et al.* (2011). Since high external pressure was used in this test, there is not much difference between top and bottom sponge resistance and

$$R = R_{measured} - 2R_{sponge} \tag{8}$$

where R is the electrical resistance of mortar cylinder, $R_{measured}$ is the measured value of the whole system and R_{sponge} is the electrical resistance of sponge.

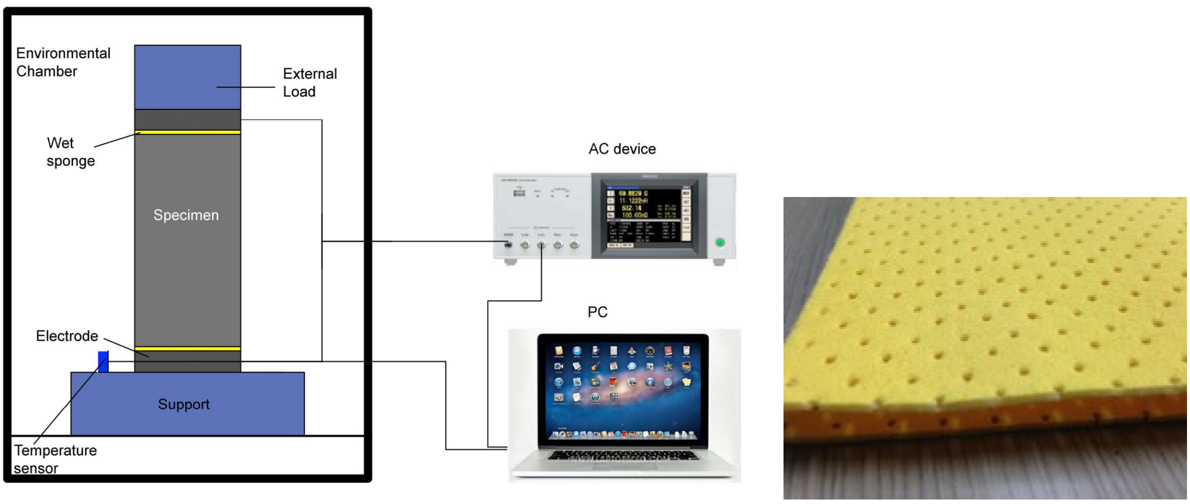

(a) (b)

Fig. 2 Setup of the test (a) Test setup (AC device is a commercial resistivity meter) (b) Details of the wet sponge.

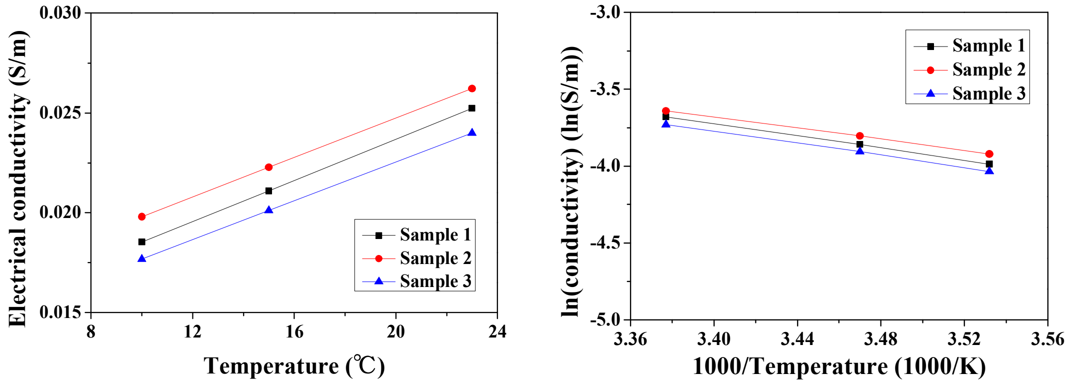

(a) (b)

Fig. 3 Relationship between electrical conductivity and temperature at full saturation.

To consider the geometrical effect, the conductivity of the specimen is

$$\sigma = \frac{1}{\rho} = \frac{1}{KR} = \frac{L}{aR} \tag{9}$$

where ρ is the resistivity of the mortar, K is the geometrical parameter, a is the cross-sectional area and L is the length of the test specimen.

3.2.2 Freeze-thaw tests

As shown in **Fig. 2**, specimens were set in the environmental chamber, which can control temperature and relative humidity. The temperature history of the environmental chamber was measured by a temperature sensor recorded by computer. The temperature cycle (Sicat *et al.* 2013) started at 10℃ for 90 minutes, then decreased by 0.25℃ per minute until it reached -28℃ and remained constant for 90 minutes, and then increased by 0.25℃ per minute until the maximum temperature 10℃. The FTC was repeated 3 times for three saturated specimens. The detailed temperature history of one cycle can be viewed from **Fig. 4**. The relative humidity in the chamber at 10℃ is around 90%. Since the specimens were sealed during the test, the relative humidity controlled in the environmental chamber had insignificant effect to the electrical conductivity of specimens.

4. Results and discussion

4.1 The activation energy at fully saturation

According to the theoretical model for calculating ice content (Eqs. (4) and (5)), only the activation energy at full saturation ($E_{a,s}$) and the saturation coefficient (n) are needed. The activation energy of the specimen is a parameter which can indicate the electrical conductivity's sensitivity to temperature, and highly depends on the degree of saturation of the specimen and the material properties. As shown in **Fig. 3**, although there is some difference between each specimen, the electrical conductivity and temperature show a linear relationship for all three specimens with similar slope values. The activation energies of the three specimens at full saturation

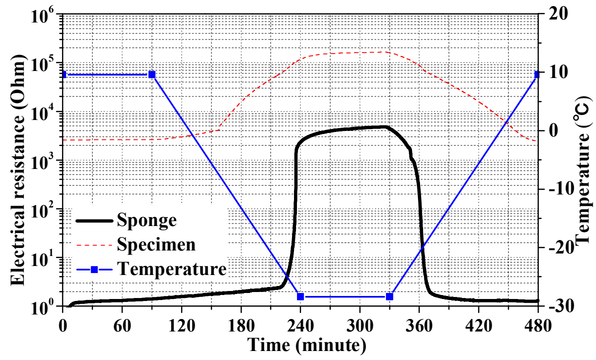

Fig. 4 Comparison of the electrical resistance of specimen and sponge under freeze-thaw cycle.

are all about 16kJ/mol, which was calculated from Eq. (A.7) with regard to the measured electrical conductivity and temperature.

4.2 The electrical resistance of sponge under FTC

As shown in **Fig. 4**, the electrical resistance of the sponge was not constant along with temperature change and it was observed negligible when the temperature is higher than -20℃. To be more exact, at temperature above zero, the electrical resistance of the wet sponge is less than 2 Ω. Due to the ice formation in the sponge at temperatures below -20℃, the electrical resistance increased exponentially though it was still very small compared with the electrical resistance of mortar. By subtracting the electrical resistance of the sponge (Eq. (8)) from the measured total electrical resistance, correct electrical resistance of mortar under FTCs was obtained.

4.3 The electrical resistivity of specimen under FTCs

Due to complexity of measuring the inside temperature of samples, only the temperature of sample surface was measured, which was found to be the same as the set temperature. According to the study of Hasan *et al.* (2003), the temperature inside a concrete cylinder with size of ϕ100mm×200mm was rather uniform. Therefore, the uniformly distributed temperature inside of the specimens was assumed in this paper because the sample size in this study is much smaller than Hasan's case. The resistivity of three specimens under three FTCs is shown in **Fig. 5**. The electrical resistivity of specimens changed dramatically in response to temperature change, especially under lower temperature. If the temperature variations are not the same during each cycle because of the change of thermal conductivity coefficient caused by frost damage, the electrical resistivity variations would be also very different. However, as can be seen in **Fig. 5**, the electrical resistivity becomes almost constant when the temperature becomes 10℃, which means that the temperature hysteresis change due to the frost damage was negligible. In addition, the temperature variation of concrete samples with FTCs was measured in (McCarter *et al.* 2015). Their temperature hysteresis results show little difference between two temperature cycles, which can also confirm that the change of thermal conductivity coefficient is not obvious after one cycle of frost damage. So it is reasonable to use the set temperature as the index of the temperature of the sample. Although there is a slight difference in resistivity between the three specimens at 10℃, their variation tendencies are almost the same, which means they have the similar ice formation process. The difference may be due to the testing scatter. The sample 3 may be slightly less porous or have lower degree of saturation than the other two. As a result, it has less frost damage and the difference becomes larger with increasing numbers of the cycles. Because the three specimens show very similar results, only the result of sample one is presented in detail in **Fig. 6** for the electrical resistivity change during freezing and thawing process for each cycle. When the temperature is above 0℃, the logarithm of electrical resistivity is in linear relationship with temperature which means the change is simply due to the temperature variation, there is no ice formation. When the temperature drops below about -7℃, the resistivity starts to increase sharply. This turning point may be interpreted as the freezing point, while the turning point of resistivity with temperature increasing at the thawing phase can also be interpreted as the thawing point. For three freeze-thaw cycles, the freezing point increases with cycles while the thawing point decreases, which was also observed by Wang *et al.* (2014) (see details in the **Fig. 7**). Generally, the freezing point of mortar is below 0℃, which may be due to the supercooling nature of mortar (Sun and Scherer 2010b). Because the supercooling phenomenon is a random phenomenon (Zeng *et al.* 2015), from the statistical point of view, the freezing point change tendency needs further experimental confirmation. In a short temperature range after the freezing point, the logarithm of electrical resistivity is in linear increasing, which means the resistivity difference is mainly due to temperature change. However, with further changing of temperature, the nonlinearity of resistivity curve is more obvious, which indicates that the ice formation is continuous under lowering temperature due to pore radius variation (water filled in smaller pores has lower freezing point) resulting in continuous decrease in liquid saturation rate. If the ice formation is instant at a certain temperature rather than being continuous, after a sudden change of slope, the curve is supposed to be linear. At the lowest temperature, the resistivity still increases to some extent, which may be caused by water re-distribution at the maintained temperature. Since the chemical potential difference caused by ice formation may induce the water to flow from

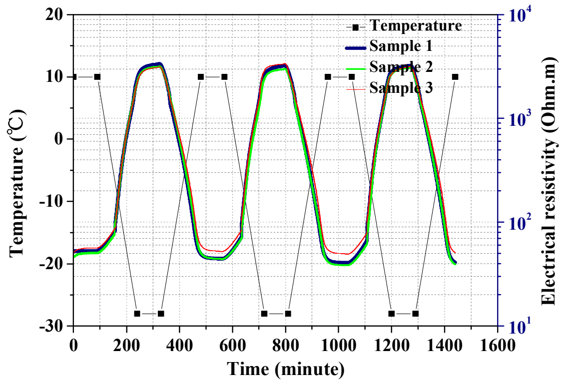

Fig. 5 Electrical resistivity changes under three freeze-thaw cycles.

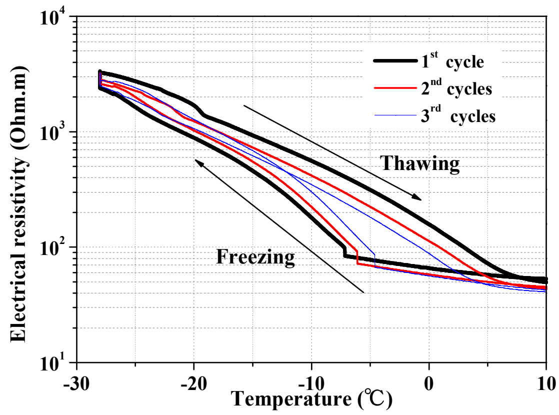

Fig. 6 Electrical resistivity changes under freezing and thawing.

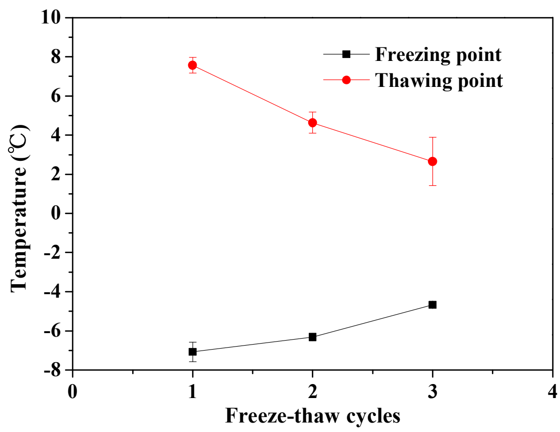

Fig. 7 Freezing and thawing points of specimens with FTCs.

smaller pores to bigger pores, the ice formation could continue even under the constant temperature. As a result, the electrical resistivity would increase due to the reduced liquid saturation degree. During the thawing process, the curve seems smoother than the freezing process because there is no supercooling effect, but the thawing point is higher than 0℃ which may be due to the size of specimen. Owing to the temperature hysteresis, the smaller the specimen size, the closer of the thawing point to 0℃. This is because the heat needs time to be transferred, if the specimen is pretty large. It may take a certain time to achieve 0℃ at the center of the specimen for thermal conducting. Therefore, the temperature at the surface of the specimen may be very different from 0℃.

4.4 Estimation of ice content in mortar under FTCs

Equations (4) and (5) are used for calculation of ice content, in which the activation energy at full saturation (16kJ/mol) was obtained from our previous test as shown in Section 4.1 and the saturation coefficient approximates to 3.5 (referred to Weiss *et al.* (2012)). From the results shown in **Fig. 8** and **Fig. 9**, under freezing, the relative ice content increases continuously after ice formation starts, reaching around 0.5 at -28℃. When the temperature was kept at -28℃, the ice content still has a slight rise. This is mainly due to the unfrozen water redistribution as a result of the chemical potential difference in pores with ice formation. During the thawing, the amount of ice content is higher than that of the freezing process at the same temperature, which is probably because of the natural supercooling effect of the porous medium. To be more precise, water in some of the pores reached the freezing point cannot form to ice due to lacking of ice nucleation crystals during freezing. However, this kind of phenomenon would not happen during thawing, which will result in the ice amount difference between the two processes. The theoretical result from ice formation analysis (Gong *et al.* 2013) based on thermodynamics and pore size distribution information of mortar (Gong *et al.* 2014) is also presented in **Fig. 8**. It seems the theoretical result agrees reasonably well with the test results if we exclude the supercooling effect, which was not considered in the theoretical results in this study. The ice content variation with FTCs is shown in **Fig. 9**. From the results of the three specimens, they show almost the same change with temperature, which confirms that the proposed method to estimate ice contents is reliable.

After revealing the ice formation process in mortar with electrical measurements, the results were compared with existing test results. Data from Sun and Scherer (2010b) was used for comparison. The study of Sun and Scherer applied a differential scanning calorimeter (DSC) to obtain the amount of ice formation in the mortar. It can be seen from **Fig. 10(a)** that the shapes of results from Sun and Scherer and our test results are similar for freezing and thawing stages. The difference probably is due to different curing conditions and specimen sizes. Firstly, specimens from Sun and Scherer were immersed into limewater for six months before the test while our specimens were cured under tap water. This means our specimens would be more porous because of Ca^+ leaching. Even though the w/c of Sun and Scherer's specimens is 0.55, the maximum value of ice content is still lower than our case (w/c=0.5). Secondly, the specimen Sun and Scherer used is 5 mm×5 mm×1 mm disk whereas our specimen is ϕ50 mm×100 mm cylinder. The reason why our specimen shows the greater difference between freezing and thawing points is the larger specimen size. The response to temperature difference, in other words, temperature hysteresis takes longer time. This point can also explain why there is slight increase in ice content during constant lowest temperature.

In addition, the relative ice content of mortar specimens with different degrees of saturation under freezing and thawing from test results of Farnam *et al.* (2015) was calculated by the proposed model. Farnam *et al.* (2015) also tested the electrical response of mortar under FTC but they used a nickel conductive coating to reduce the interface effect between electrodes and specimen instead of wet sponges. Besides, by following ASTM C305-12, the mortar samples were sealed to cure

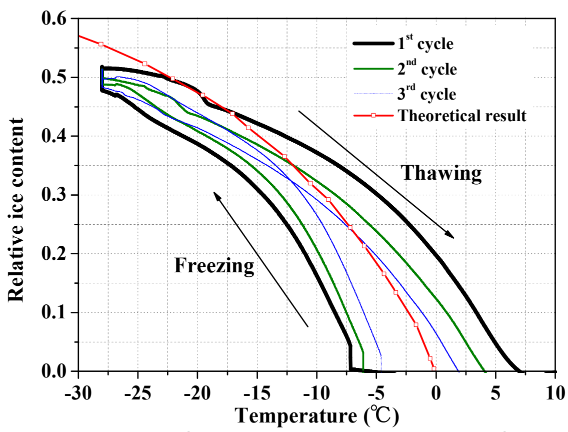

Fig. 8 Estimation of relative ice content in case of n=3.5 (Weiss *et al.* 2012).

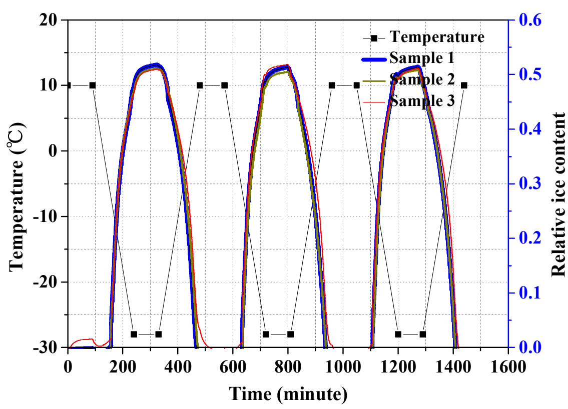

Fig. 9 Estimation of relative ice content with FTCs.

for 28 days. Since they used relatively small size specimens (25.4 mm×25.4 mm×50.8 mm) in comparison with our specimen, the difference in relative ice content between freezing and thawing process is smaller than our case as shown in **Fig. 10(b)**. Because the energetic barrier to nucleation may vary with sample sizes (Sun and Scherer 2010a), the ice formation processes varied accordingly. Although the shape and the tendency of the curves are similar, the maximum relative ice content in Farnam *et al*'s test is less than 0.5 for a fully saturated specimen. The reason may be explained by the lower water to cement ratio (0.42).

Furthermore, the calculated relative ice content of the different saturated specimens are shown in **Fig. 11(a)** and compared to the theoretical results (w/c=0.42 was used) from Gong *et al.* (2013) in **Fig. 11(b)** for the freezing process. It seems that the results have an acceptable agreement. Even though there is a slight difference at temperature near to the freezing point due to supercooling effect and lower than -20℃ due to possibly ice percolation, the model can reasonably predict the ice formation in partially saturated cases.

4.5 Estimation of ice content with consideration of frost damage

It is common understanding that the frost damage may change the microstructural characteristics of mortar (e.g. porosity and connectivity), therefore electrical resistivity of mortar may be affected as well. As a consequence, electrical conductivity of fully saturated mortar at the reference temperature $\sigma_{ref,s}$, activation energy of fully saturated concrete for the conduction process $E_{a,s}$ and saturation coefficient n (see Eq. (1)) would be different before and after FTC. Among them, $E_{a,s}$ and n are correlated with $\sigma_{ref,s}$. Therefore, the change of $\sigma_{ref,s}$ may represent the damage effect and this is the basic concept for Eq. (6). The frost damage does not suddenly happen but is accumulated with FTCs, which needs cycles to be serious. It may be ignored within one cycle for estimating relative ice content. As it is shown in **Fig. 12** where the electrical data is cited from Farnam *et al.* (2015), and the damage evolution is assumed to be linear with temperature variation during freezing phase, the estimated relative ice content with and without considering frost damage does not show much difference within one cycle. To evaluate ice content more precisely during

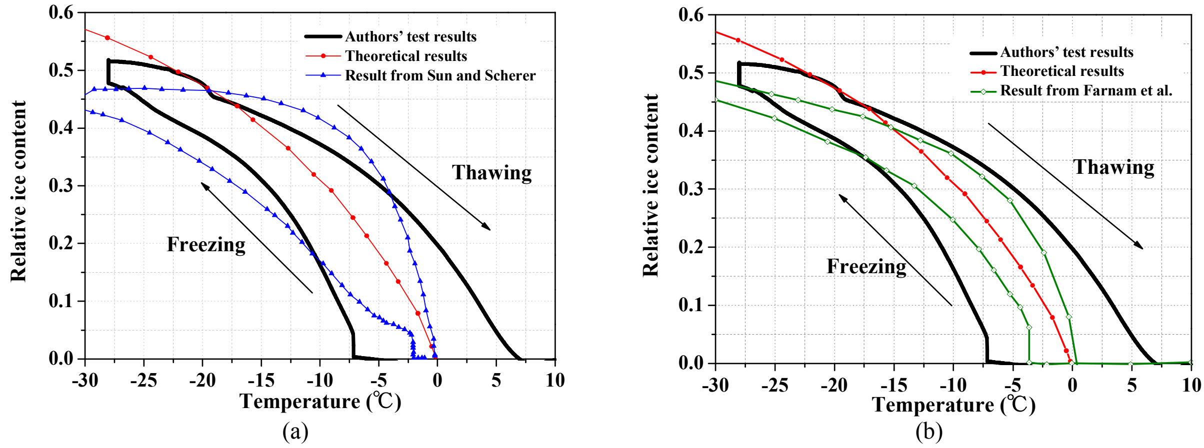

Fig. 10 Comparison ice content of mortar obtained from (a) electrical test (authors') and calorimetric test (Sun and Scherer, 2010) and (b) electrical test (authors' and Farnam *et al.*, 2015) (calculated by the author's model).

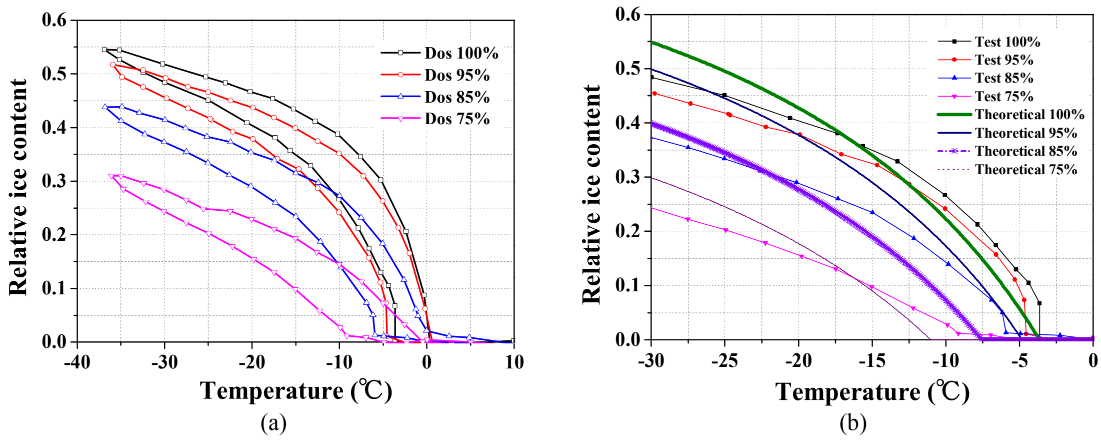

Fig. 11 Calculated relative ice content from electrical test results of Farnam *et al.* (2015) by using authors' model (a) Relative ice content of different degree of saturation under freezing and thawing (b) Comparison of the test results and theoretical results from Gong *et al.* (2013a).

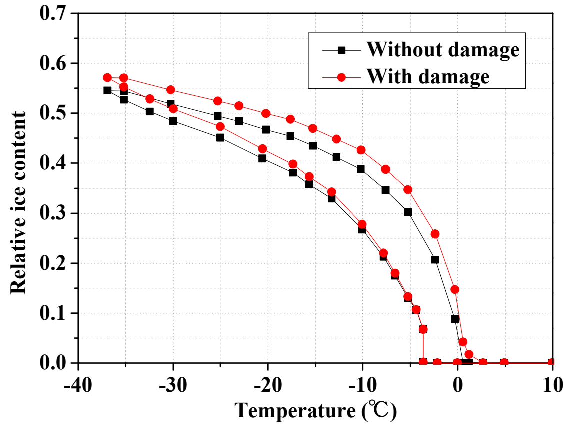

Fig. 12 Calculated relative ice content from test results (fully saturated case) of Farnam *et al.* (2015) by using authors' model with and without considering frost damage development.

thawing process, we need for further experimentation to investigate the effects of damage on electrical conductivity. And further verification is necessary under multiple FTCs.

5. Conclusions

(1) The combined effect of temperature and moisture content on electrical conductivity of concrete is explained from a theoretical point of view. Under freezing conditions, the two effects both play significant roles in the electrical behavior of concrete and the interactive effect is more obvious under higher temperatures and higher degrees of saturation. In this study, the relationship between the activation energy and the degree of saturation is derived. A method to estimate the ice content based on electrical measurements is proposed considering the coupled effect of temperature and moisture content. Although the ice formation in partially saturated specimens was calculated for one cycle based on the test results of Farnam *et al.* (2015), the proposed model still needs further experimental study with multiple FTCs for the verification of applicability.

(2) Based on the proposed method, the relative ice content of mortar is estimated by conducting the electrical test. The test results of three samples during FTCs are consistent and the ice formation process is continuous with temperature variation, which means the proposed test method is reliable and repeatable. The freezing point of specimen is increasing with cycles while the thawing point has an opposite tendency. In addition, during FTCs, the relative ice content (the mass ratio of frozen water content to the total water content in mortar) during thawing is higher than that of freezing under the same temperature. The maximum value for the samples is around 0.5 at temperature -28℃. These results can be useful for the prediction of frost damage of concrete (Gong *et al.* 2015a).

(3) The calculated ice content from the developed model is compared with theoretical result from thermodynamic analysis and found in acceptable agreement with each other. The calculated ice content is also compared with existing experimental results of other researchers', which were based on calorimetric test and electrical test data interpreted with this study's model. The shape of ice content and temperature curves looks similar. The difference in ice contents between our test and the existing tests can be explained by difference in material properties and curing condition. The frost damage of mortar to electrical conductivity is also discussed and concluded that the damage effect may be ignored within one FTC for estimating ice formation because the frost damage is cumulative and it is not so significant for a cycle. These verify the reliability and applicability of the proposed model.

Acknowledgement

The authors would like to express their sincere thanks to the Grant-in-Aid for Scientific Research (A) of Japan Society of Promotion of Science (No. 26249064). The first author would also like to show his gratitude to the scholarship granted by Chinese Scholarship Council (CSC) which supports the author's PhD study and research work. The authors are also greatly indebted to Prof. Jason Weiss and Mr. Robert Spragg (Purdue University) for their advice during this study.

Appendix. Normalized electrical conductivity ($\sigma_{T,p}/\sigma_{ref,s}$)

Normalized electrical conductivity $\sigma_{T,p}/\sigma_{ref,s}$ (electrical conductivity of partially saturated specimen at temperature T slash electrical conductivity of fully saturated specimen at reference temperature T_{ref}) is vitally important for estimating the ice content and it can be derived as following

$$\frac{\sigma_{ref,p}}{\sigma_{ref,s}} = S^n \tag{A.1}$$

$$\frac{\sigma_{T,p}}{\sigma_{ref,s}} = \frac{\sigma_{T,p}}{\sigma_{ref,p}\cdot S^{-n}} = \frac{\sigma_{T,p}}{\sigma_{ref,p}}\cdot S^n \tag{A.2}$$

where $\sigma_{ref,s}$ is the electrical conductivity of fully saturated concrete at the reference temperature T_{ref}, $\sigma_{ref,p}$ is the electrical conductivity of partially saturated concrete at the reference temperature (the same degree of saturation with measured one at temperature T (K)) and $\sigma_{T,p}$ is the electrical conductivity of partially saturated concrete at the absolute temperature T.

By substituting of Eq. (3) into (A.2), the normalized electrical conductivity would be

$$\frac{\sigma_{T,p}}{\sigma_{ref,s}} = e^{-\left[\frac{E_{a,p}}{R_g}\left(\frac{1}{T}-\frac{1}{T_{ref}}\right)\right]}\cdot S^n \tag{A.3}$$

where $E_{a,p}$ is the activation energy of partially saturated concrete for the conduction process.

From Eq. (A.3), the activation energy of partially saturated concrete for the conduction process may be calculated as following

$$e^{-\left[\frac{E_{a,p}}{R_g}\left(\frac{1}{T}-\frac{1}{T_{ref}}\right)\right]} = \frac{\sigma_{T,p}}{\sigma_{ref,s}} \cdot S^{-n} \tag{A.4}$$

$$\frac{E_{a,p}}{R_g}\left(\frac{1}{T}-\frac{1}{T_{ref}}\right) = \ln\left(S^n\right) - \ln\left(\frac{\sigma_{T,p}}{\sigma_{ref,s}}\right) \tag{A.5}$$

$$E_{a,p} = \frac{R_g}{\left(\frac{1}{T}-\frac{1}{T_{ref}}\right)} \cdot \left[\ln\left(S^n\right) - \ln\left(\frac{\sigma_{T,p}}{\sigma_{ref,s}}\right)\right] \tag{A.6}$$

When saturation degree S=1, then

$$E_{a,s} = -\frac{R_g \ln\left(\frac{\sigma_{T,s}}{\sigma_{ref,s}}\right)}{\frac{1}{T}-\frac{1}{T_{ref}}} \tag{A.7}$$

where $E_{a,s}$ is the activation energy of fully saturated concrete for the conduction process, $\sigma_{T,s}$ is the electrical conductivity of fully saturated concrete at the absolute temperature T.

Eqs. (A6)and (A7) are functions to calculate the activation energy only. Although there is a temperature parameter in the equations, it does not mean that the activation energy is dependent on temperature since $\sigma_{T,s}$ and $\sigma_{T,p}$ will change with temperature so the temperature parameter can be removed finally.

Besides, the normalized value $\sigma_{T,p}/\sigma_{ref,s}$ can also be calculated based on Eq. (2) directly:

$$\sigma_{T,p} = A_p e^{-\left(\frac{E_{a,p}}{R_g T}\right)} \tag{A.8}$$

$$\sigma_{ref,s} = A_s e^{-\left(\frac{E_{a,s}}{R_g T_{ref}}\right)} \tag{A.9}$$

where A_p is the nominal conductivity at infinite temperature at the measured degree of saturation, A_s is the nominal conductivity at infinite temperature at the fully saturation.

From Liu and Presuel-Moreno (2014), the value of A fluctuates with different degrees of saturation was found, but the difference was not significant (see details in (Wang *et al.* 2014)). So this value is assumed to be constant. By dividing Eq. (A.8) with Eq. (A.9), if A_p=A_s is assumed here, then

$$\frac{\sigma_{T,p}}{\sigma_{ref,s}} = e^{-\left[\frac{E_{a,p}}{R_g T}-\frac{E_{a,s}}{R_g T_{ref}}\right]} \tag{A.10}$$

By combining Eqs. (A.3) and (A.10), the relationship between activation energy for fully saturated and partially saturated specimen may be rewritten as following

$$e^{-\left[\frac{E_{a,p}}{R_g}\left(\frac{1}{T}-\frac{1}{T_{ref}}\right)\right]} \cdot S^n = e^{-\left[\frac{E_{a,p}}{R_g T}-\frac{E_{a,s}}{R_g T_{ref}}\right]} \tag{A.11}$$

$$e^{-\left[\frac{E_{a,p}}{R_g T}-\frac{E_{a,s}}{R_g T_{ref}}-\frac{E_{a,p}}{R_g T}+\frac{E_{a,p}}{R_g T_{ref}}\right]} = S^n \tag{A.12}$$

$$e^{-\left(\frac{E_{a,p}-E_{a,s}}{R_g T_{ref}}\right)} = S^n \tag{A.13}$$

$$E_{a,p} = E_{a,s} - R_g T_{ref} \ln\left(S^n\right) \tag{A.14}$$

Finally, by substituting Eq. (A.14) into Eq. (A.3), the normalized electrical conductivity is

$$\frac{\sigma_{T,p}}{\sigma_{ref,s}} = e^{-\left[\frac{E_{a,s}-R_g T_{ref}\ln\left(S^n\right)}{R_g}\left(\frac{1}{T}-\frac{1}{T_{ref}}\right)\right]} \cdot S^n \tag{A.15}$$

References

Archie, G. E., (1942). "The electrical resistivity log as an aid in determining some reservoir characteristics." *Transactions of the AIME*, 146(01), 54-62.

Cai, H. and Liu, X., (1998). "Freeze-thaw durability of concrete: ice formation process in pores." *Cement and Concrete Research*, 28(9), 1281-1287.

Chrisp, T., Starrs, G., McCarter, W., Rouchotas, E. and Blewett, J., (2001). "Temperature-conductivity relationships for concrete: An activation energy approach." *Journal of materials science letters*, 20(12), 1085-1087.

Farnam, Y., Todak, H., Spragg, R. and Weiss, J., (2015). "Electrical response of mortar with different degrees of saturation and deicing salt solutions during freezing and thawing." *Cement and Concrete Composites*, 59(0), 49-59.

Gong, F., Sicat, E., Ueda, T. and Zhang, D., (2013). "Meso-scale Mechanical Model for Mortar Deformation under Freeze Thaw Cycles." *Journal of Advanced Concrete Technology*, 11(2), 49-60.

Gong, F., Zhang, D., Sicat, E. and Ueda, T., (2014). "Empirical estimation of pore size distribution in cement, mortar, and concrete." *Journal of Materials in Civil Engineering*, 26(7), 04014023.

Gong, F., Sicat, E., Zhang, D. and Ueda, T., (2015a). "Stress analysis for concrete materials under multiple freeze-thaw cycles." *Journal of Advanced Concrete Technology*, 13(3), 124-134.

Gong, F., Wang, Y., Zhang, D. and Ueda, T., (2015b). "Mesoscale simulation of deformation for mortar and concrete under cyclic freezing and thawing stress." *Journal of Advanced Concrete Technology*, 13(6), 291-304.

Hasan, M., Okuyama, H. and Ueda, T., (2003). "The damage mechanism and strain induced in frost cycles of concrete." *Proceedings of the Japan Concrete Institute*, 25(1), 401-406.

Johannesson, B, (2010). "Dimensional and ice content changes of hardened concrete at different freezing and thawing temperatures." *Cement and Concrete Composites*, 32(1), 73-83.

Kjeldsen, A. M. and Geiker, M. R., (2008). "On the interpretation of low temperature calorimetry data." *Materials and Structures*, 41(1), 213-224.

Katsura, O., Yoshino, T. and Kamada, E., (1996). "Estimation of frozen water in cementitious material and dependence of ice formation on pore structure." *Concrete Research and Technology*, 7(1), 57-66. (in Japanese)

Liu, Y. and Presuel-Moreno, F. J., (2014). "Normalization of temperature effect on concrete resistivity by method using Arrhenius law." *ACI Materials Journal*, 111(1-6).

McCarter, W., Starrs, G., Chrisp, T., Basheer, P., Nanukuttan, S. and Srinivasan, S., (2015). "Conductivity/activation energy relationships for cement-based materials undergoing cyclic thermal excursions." *Journal of Materials Science*, 50(3), 1129-1140.

Newlands, M. D., Jones, M. R., Kandasami, S. and Harrison, T. A., (2008). "Sensitivity of electrode contact solutions and contact pressure in assessing electrical resistivity of concrete." *Materials and Structures*, 41(4), 621-632.

Powers, T. C., (1945). "A working hypothesis for further studies of frost resistance of concrete." *ACI journal Proceedings*, ACI, 41(1).

Petrenko, V. F., (1993). "*Electrical properties of ice*." Cold Regions Research and Engineering Lab Hanover NH.

Perron, S. and Beaudoin, J., (2002). "Freezing of water in portland cement paste-an ac impedance spectroscopy study." *Cement and Concrete Composites*, 24(5), 467-475.

Panchmatia, P., Olek, J., Whiting, N., Byers, M. and Nantung, T., (2014). "Concrete conductivity: Effects of temperature, saturation and air content."

Rajabipour, F. and Weiss, J., (2007). "Electrical conductivity of drying cement paste." *Materials and Structures*, 40(10), 1143-1160.

Scherer, G. W. and Valenza II, J. J., (2005). "Mechanisms of frost damage." *Materials science of concrete*, 7, 209-246.

Sun, Z. and Scherer, G. W., (2010a). "Effect of air voids on salt scaling and internal freezing." *Cement and Concrete Research*, 40(2), 260-270.

Sun, Z. and Scherer, G. W., (2010b). "Pore size and shape in mortar by thermoporometry." *Cement and Concrete Research*, 40(5), 740-751.

Sato, T. and Beaudoin, J. J., (2011). "Coupled AC impedance and thermomechanical analysis of freezing phenomena in cement paste." *Materials and structures*, 44(2), 405-414.

Spragg, R. P., Castro, J., Nantung, T. E., Paredes, M. and Weiss, W. J., (2011). "Variability analysis of the bulk resistivity measured using concrete cylinders." *Joint Transportation Research Program, Indiana Department of Transportation and Purdue University, West Lafayette, Indiana.*

Spragg, R. P., Castro, J., Nantung, T., Paredes, M. and Weiss, J., (2012). "Variability analysis of the bulk resistivity measured using concrete cylinders." *Advances in Civil Engineering Materials*, 1(1), 104596.

Spragg, R., Bu, Y., Snyder, K., Bentz, D. and Weiss, J., (2013). "*Electrical testing of cement-based materials: Role of testing techniques, sample conditioning, and accelerated curing*." Joint Transportation Research Program, Indiana Department of Transportation and Purdue University*, West Lafayette, Indiana*.

Sicat, E., Gong, F., Zhang, D. and Ueda, T., (2013). "Change of the coefficient of thermal Expansion of mortar due to damage by freeze thaw cycles." *Journal of Advanced Concrete Technology*, 11(12), 333-346.

Valenza, J. J. and Scherer, G. W., (2007). "A review of salt scaling: II. Mechanisms." *Cement and Concrete Research*, 37(7), 1022-1034.

Villagrán Zaccardi, Y., Fullea García, J., Huelamo, P. and Di Maio, A., (2009). "Influence of temperature and humidity on Portland cement mortar resistivity monitored with inner sensors." *Materials and corrosion*, 60(4), 294-299.

Whittington H. W., McCarter J. and Forde M. C., (1981). "The conduction of electricity through concrete." *Magazine of concrete research*, 33(114), 48-60.

Weiss, J., Snyder, K., Bullard, J. and Bentz, D., (2012). "Using a saturation function to interpret the electrical properties of partially saturated concrete." *Journal of Materials in Civil Engineering*, 25(8), 1097-1106.

Wang, Z., Zeng, Q., Wang, L., Yao, Y. and Li, K., (2014). "Effect of moisture content on freeze–thaw behavior of cement paste by electrical resistance measurements." *Journal of Materials Science*, 49(12), 4305-4314.

Wang, Z., Zeng, Q., Wang, L., Yao, Y. and Li, K., (2015). "Electrical resistivity of cement pastes undergoing cyclic freeze-thaw action." *Journal of Materials in Civil Engineering*, 27(1), 04014109.

Wang, Y., Gong, F., Ueda, T. and Zhang, D., (2014). "Theoretical model for estimation of ice content of concrete by using electrical measurements." *Procedia Engineering*, 95(0), 366-375.

Zeng, Q., Li, K. and Fen-Chong, T., (2015). "Heterogeneous nucleation of ice from supercooled NaCl solution confined in porous cement paste." *Journal of Crystal Growth*, 409, 1-9.

Notations

σ_c :Electrical conductivity of partially saturated concrete (S/m)
σ_{cs} :Electrical conductivity of fully saturated concrete (S/m)
σ :Electrical conductivity at the absolute temperature T (K) (S/m)
σ_{ref} :Electrical conductivity at absolute reference temperature T_{ref} (the measured one and the reference one are the same degree of saturation) (S/m)
$\sigma_{ref,s}$:Electrical conductivity of fully saturated concrete at the reference temperature T_{ref} (S/m)
$\sigma_{refi,s}$:Electrical conductivity of fully saturation concrete at the reference temperature before the i cycle
$\sigma_{refi+1,s}$:Electrical conductivity of fully saturation concrete at the reference temperature after the i cycle
$\sigma_{ref,p}$:Electrical conductivity of partially saturated concrete at the reference temperature T_{ref} (S/m)
$\sigma_{T,p}$:Electrical conductivity of partially saturated concrete at the absolute temperature T (S/m)
T_{ref} :Reference temperature (K) (296K in this paper)
T :Measured absolute temperature (K)
T_F :Freezing point (K)
T_L :Lowest temperature (K)
S :Degree of saturation of concrete
S_{iF} :Unfrozen water content during freezing at a certain i cycle
S_{iT} :Unfrozen water content during thawing at a certain i cycle
n :Saturation coefficient which is determined by the intrinsic properties of concrete such as porosity and connectivity and chemical composition of pore solution
A :Nominal conductivity at infinite temperature ($T\to\infty$)(S/m)
A_p :Nominal conductivity at infinite temperature with partially saturation (S/m)
A_s :Nominal conductivity at infinite temperature with the fully saturation (S/m)
R_g :Universal gas constant (8.314 J/mol/K)
E_a :Activation energy for the conduction process (kJ/mol)
$E_{a,p}$:Activation energy of partially saturated concrete for the conduction process (kJ/mol)
$E_{a,s}$:Activation energy of fully saturated concrete for the conduction process (kJ/mol)
R :Electrical resistance of mortar cylinder (Ω)
$R_{measured}$:Measured value of the whole system (Ω)
R_{sponge} :Electrical resistance of sponge (Ω)
ρ :Resistivity of the mortar (Ω.m)
K :Geometrical parameter
a :Cross-sectional area (m^2)
L :Length of the test specimen (m)